Major Element Variation and Possible Source Materials of Apollo 12 Crystalline Rocks

Abstract. *Nine different crystalline rocks of the Apollo 12 samples have been analyzed with conventional chemical rock analysis methods. Five of the rocks have normative quartz, whereas the others have normative olivine and hypersthene. The rocks show a wide range in the ratio of iron to magnesium, and their compositions fall on relatively smooth curves in the oxide variation diagram. It is suggested that these rocks, with one exception, represent different parts of a differentiated magmatic body, in which magmatic differentiation by crystallization and settling of olivine was most effective. The source material of the original magma may be peridotite with or without minor amounts of plagioclase or spinel or garnet, with the presence or absence of these minerals dependent on the depth of magma generation.*

As part of the petrological studies on the Apollo 12 rocks, nine different crystalline rocks [12018-60, 12020-47, 12021-86, 12022-98, 12038-54, 12040-31, 12052-76, 12064-31, and 12065 (45 and 79)] have been analyzed with conventional chemical rock analysis methods. The results of the analyses are given in Table 1. About 1 g of sample was used for each analysis. Except for sample 12065, single analyses only were made on 25 to 50 g of crushed, ground, and homogenized material. Two portions of sample 12065, one of 25 g (sample 12065-79) and the other representing a 3.10-g chip, were analyzed separately. Two analyses were carried out because the analytical result first obtained for sample 12065 was considerably different from that reported by the Lunar Sample Preliminary Examination Team (*1*), chiefly in the SiO_2 value, and a second analysis was made on a separate portion of the same rock specimen to verify the first result. The content of P_2O_5 is much higher in the small rock chip than in the homogenized portion of the larger rock chip, probably because of the local concentration of apatite in the small chip. Ferric iron and H_2O^- were not detected in any of the samples analyzed; H_2O^+ was not determined. Petrographical descriptions of four of the analyzed rocks will be presented elsewhere (*2*).

Norms calculated from these analyses are shown in Table 1. Five of the analyzed samples have normative quartz, whereas the others have normative olivine and hypersthene. The quartz-normative rocks are similar to iron-rich tholeiite and the olivine-normative rocks are similar to olivine-rich tholeiite, although the content of TiO_2 is higher and that of alkalies is lower in the analyzed rocks than in most tholeiites.

The new analyses are plotted in the oxide variation diagram (Fig. 1) together with the analyses of the Apollo 11 crystalline rocks (*3*) and some of the preliminary analyses of the Apollo 12 crystalline rocks (*1*). The horizontal axis of this diagram is the solidification index of Kuno *et al.* (*4*), which is one measure of the degree of fractional crystallization represented, and which indicates the degree of solidification of terrestrial magmas (*5*). The Apollo 12 crystalline rocks have a wider range in

Table 1. Chemical compositions and norms [in percentage (by weight)] of Apollo 12 crystalline rocks.* Q, quartz; Or, orthoclase; Ab, albite; An, anorthite; Wo, wollastonite; En, enstatite; Fs, ferrosilite; Di, diopside; Fo, forsterite; Fa, fayalite; Ol, olivine; Hy, hypersthene; Il, ilmenite; Cm, chromite; Ap, apatite.

Component	Rock sample									
	12018-60	12020-47	12021-86	12022-98	12038-54	12040-31	12052-76	12064-31	12065-45	12065-79
					Chemical composition					
SiO_2	43.89	44.45	46.46	42.33	47.05	43.68	46.49	46.19	46.61	46.14
TiO_2	2.56	2.54	3.44	4.54	3.22	2.48	3.18	3.83	3.15	3.34
Al_2O_3	8.20	7.99	10.55	9.12	12.12	7.35	10.29	10.96	10.58	10.73
Cr_2O_3	0.66	0.68	0.40	0.56	0.34	0.70	0.55	0.36	0.48	0.47
Fe_2O_3	0.0	0.0	0.0	0.0	0.0	0.0	0.0	0.0	0.0	0.0
FeO	20.56	20.65	19.68	22.06	17.91	20.91	19.93	19.83	19.36	19.86
MnO	0.25	0.26	0.26	0.26	0.24	0.26	0.27	0.26	0.26	0.26
MgO	15.54	14.89	7.60	11.58	7.09	16.69	8.44	6.60	8.04	8.05
CaO	8.21	8.53	11.37	9.37	11.46	7.91	10.82	11.84	11.13	10.96
Na_2O	0.20	0.21	0.35	0.29	0.64	0.16	0.28	0.27	0.34	0.25
K_2O	0.05	0.06	0.07	0.07	0.07	0.05	0.07	0.07	0.08	0.07
H_2O^-	0.0	0.0	0.0	0.0	0.0	0.0	0.0	0.0	0.0	0.0
P_2O_5	0.02	0.02	0.01	0.02	0.02	0.02	0.03	0.02	0.21	0.02
Total	100.14	100.28	100.19	100.20	100.16	100.21	100.35	100.23	100.24	100.15
					Norms					
Q			0.92		1.17		0.47	1.93	1.00	0.56
Or	0.28	0.33	0.39	0.39	0.39	0.28	0.39	0.39	0.50	0.39
Ab	1.68	1.77	2.98	2.46	5.39	1.36	2.35	2.30	2.87	2.10
An	21.30	20.63	26.95	23.35	29.96	19.15	26.52	28.41	27.01	27.94
Di Wo	8.05	8.96	12.21	9.53	11.15	8.32	11.18	12.56	11.14	10.96
Di En	4.20	4.59	4.74	3.96	4.39	4.13	4.52	4.52	4.47	4.32
Di Fs	3.62	4.16	7.65	5.62	6.90	4.03	6.76	8.33	6.79	6.77
Hy En	15.93	16.48	14.15	12.24	13.23	15.70	16.41	11.88	15.50	15.69
Hy Fs	13.77	14.95	22.88	13.45	20.79	12.66	24.50	21.86	23.55	24.22
Ol Fo	12.97	11.14		8.82		15.17				
Ol Fa	12.35	11.14		10.72		13.46				
Il	4.85	4.82	6.52	8.60	6.11	4.69	6.02	7.25	5.96	6.33
Cm	0.96	1.01	0.58	0.83	0.49	1.03	0.81	0.54	0.72	0.69
Ap	0.03	0.03	0.03	0.03	0.03	0.03	0.07	0.03	0.49	0.03

* Determination made by conventional chemical rock analysis methods (H. Haramura, analyst).

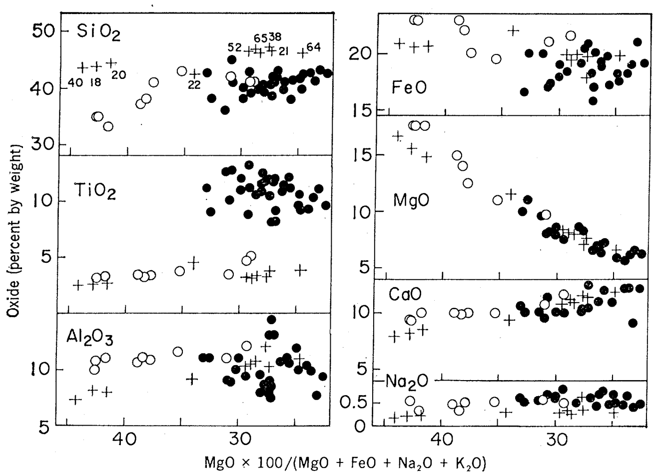

Fig. 1. Oxide variation as a function of the solidification index (*4*) of the Apollo 11 and Apollo 12 crystalline rocks. (Crosses) Apollo 12 crystalline rocks analyzed in the study reported here; (open circles) Apollo 12 crystalline rocks analyzed by the Lunar Sample Preliminary Examination Team (*1*); (solid circles) Apollo 11 crystalline rocks (*3*).

the solidification index than the Apollo 11 crystalline rocks.

The new analyses, except that for sample 12022, plot on relatively smooth curves in most of the oxide variation diagrams; the variation trend of SiO_2, TiO_2, Al_2O_3, CaO, and Na_2O increases with the decrease of the solidification index, whereas that of FeO and MgO decreases. The preliminary analyses of the Apollo 12 crystalline rocks (*1*) show the same variation trends, although the points are more scattered. This may indicate that the Apollo 12 crystalline rocks are genetically related to each other; for example, they are the crystallization products of the same or similar original magma or the partial melting products of the same original rock.

The major oxides [>1 percent (by weight)] of the analyzed crystalline rocks are plotted against the percent (by weight) of SiO_2 (Fig. 2). The composition of the most magnesian olivine [$Fo_{74}Fa_{26}$, where Fo represents forsterite and Fa represents fayalite, in mole percent with 0.26 percent (by weight) CaO and 0.35 percent (by weight) Cr_2O_3] in a Mg-rich rock 12020 (*6*) is also shown in Fig. 2. The compositions of all the analyzed rocks except that of sample 12022 fall very near the straight lines originating from the composition of $Fo_{74}Fa_{26}$ olivine in all the major oxide variation diagrams. This evidence strongly suggests that the compositions of the analyzed crystalline rocks are controlled by olivine with a composition of about $Fo_{74}Fa_{26}$. One possible explanation for this correspondence is that magmatic differentiation caused mainly by crystal settling of olivine took place in a single intrusive magmatic body or a lava lake. As shown in Fig. 2, the analyzed rocks except sample 12022 are plotted in two different compositional areas. One group (samples 12018, 12020, and 12040) may have been enriched in olivine, whereas the other group (samples 12021, 12038, 12052, 12064, and 12065) may have been relatively depleted in olivine by crystal settling. The magmatic body that was thus differentiated and solidified may have been broken by later meteorite impact, and various parts of the body may have been thrown out on the surface as rock fragments. Remelting by impact and rapid recrystallization may have occurred, but without any significant change in the original compositions. Rock 12022, whose composition does not fit the variation trends for other samples, would have been derived from a different magmatic body.

The Apollo 11 crystalline rocks plot in the area of low solidification index of the variation trends of the Apollo 12 rocks (Fig. 1). However, the content of TiO_2 is much lower and that of SiO_2 is higher in the present analyses than in the Apollo 11 rocks for the same solidification index. These differences suggest that the Apollo 11 and Apollo 12 crystalline rocks have not been derived from the same or similar original magma by a simple crystallization process, or from the same original materials by a simple partial melting process.

The composition of the original magma of the analyzed Apollo 12 crystalline rocks cannot be determined with certainty from the present analyses. If the olivine-rich group shown in Fig. 2 represents olivine cumulate (olivine-enriched) rock and the olivine-poor group represents olivine-depleted rock, as mentioned above, the original magma of the analyzed crystalline rocks except sample 12022 must have a composition between those of these two groups, and its content of each oxide must fit each of the corresponding straight lines of Fig. 2. A possible composition of the

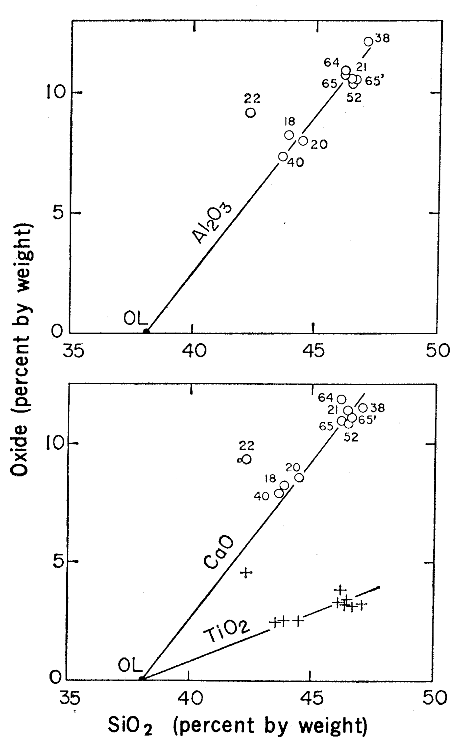

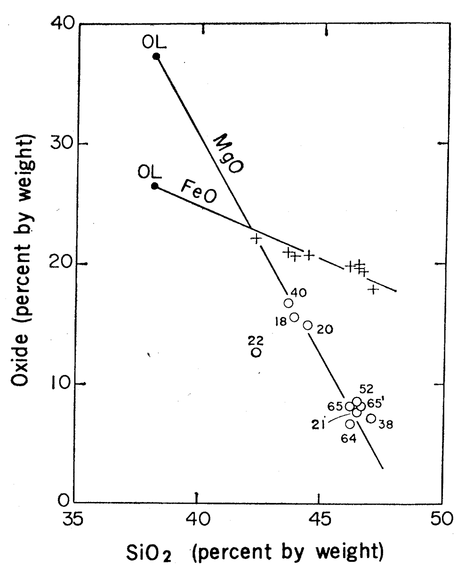

Fig. 2. Oxide variation as a function of the SiO_2 content [in percentage (by weight)] of the Apollo 12 crystalline rocks analyzed in the study reported here (crosses and open circles). Numbers are the last two digits of the Apollo 12 sample numbers given by the Lunar Sample Preliminary Examination Team; OL is the composition of the most magnesian olivine ($Fo_{74}Fa_{26}$) in rock 12020 determined with the microprobe (solid circles) (*6*). Number 65 is sample 12065-79 and number 65′ is sample 12065-45.

original magma is estimated below from Fig. 2 on the assumption that its composition [in percentage (by weight)] lies near the middle of the two groups: SiO_2, 46.0; TiO_2, 3.0; Al_2O_3, 9.7; Cr_2O_3, 0.60; FeO, 20.0; MnO, 0.25; MgO, 10.2; CaO, 10.0; Na_2O, 0.27; and K_2O, 0.06 (*7*). The composition is considerably richer in FeO and poorer in alkalies than that of the terrestrial basalts with similar MgO contents. If the magma of this composition was formed by partial melting of the moon's interior at depths less than about 200 km, the source material was most likely plagioclase-bearing peridotite or ilmenite-bearing olivine gabbro. If the magma originated at depths where plagioclase is not stable, the source material may have been peridotite containing garnet or spinel plus pyroxene solid solution with considerable amounts of Al, Ti, and Na.

IKUO KUSHIRO
HIROSHI HARAMURA
Geological Institute, University of Tokyo, Tokyo, Japan

References and Notes

1. Lunar Sample Preliminary Examination Team, *Science* **167**, 1325 (1970).
2. I. Kushiro, Y. Nakamura, K. Kitayama, S. Akimoto, in preparation.
3. S. O. Agrell, J. H. Scoon, I. D. Muir, J. V. P. Long, J. D. C. McConnell, A. Peckett, *Geochim. Cosmochim. Acta* **1** (Suppl. 1), 93 (1970); C. Frondel, C. Klein, J. Ito, J. C. Drake, *ibid.*, p. 445; H. Haramura, Y. Nakamura, I. Kushiro, *ibid.*, p. 539; I. Kushiro and Y. Nakamura, *ibid.*, p. 607; W. Compston, B. W. Chappell, P. A. Arriens, M. J. Vernon, *ibid.* **2** (Suppl. 1), 1007 (1970); A. E. J. Engel and C. G. Engel, *ibid.*, p. 1081; J. A. Maxwell, L. C. Peck, H. B. Wiik, *ibid.*, p. 1369; H. J. Rose, Jr., F. Cuttitta, E. J. Dwornik, M. K. Carron, R. P. Christian, J. R. Lindsay, D. T. Ligon, R. R. Larson, *ibid.*, p. 1493.
4. H. Kuno, K. Yamasaki, C. Iida, K. Nagashima, *Jap. J. Geol. Geogr.* **38**, 179 (1957).
5. The Apollo 11 and Apollo 12 rocks contain relatively small amounts of alkalies and this index is nearly the same as the percentage (by weight) of MgO relative to MgO plus FeO.
6. The most magnesian olivine in a relatively Mg-poor rock (sample 12065) has the composition $Fo_{71}Fa_{29}$, which is not much different from that of sample 12020 and plots close to OL in Fig. 2.
7. Plots for Cr_2O_3, MnO, and K_2O have also been made, although they are not shown in Fig. 2; values midway between those for the olivine-rich group and those for the olivine-depleted group have been obtained for these oxides.
8. We thank Dr. Y. Nakamura for helpful discussions.

28 September 1970; revised 16 November 1970 ■

Solar Particle Tracks in Glass from the Surveyor 3 Spacecraft

Abstract. *A glass filter from Surveyor 3 has a surface density of* $\sim 1 \times 10^6$ *tracks per square centimeter from heavy solar flare particles. The variation with depth is best fitted with a solar particle spectrum* $dN/dE = 2.42 \times 10^6 E^{-2}$ *[in particles per square centimeter per year per steradian per (million electron volts per nucleon)], where* E *is the energy and* N *is the number of particles, from 2 million electron volts per nucleon to* ~ 7 *million electron volts per nucleon and* $dN/dE = 1.17 \times 10^7 E^{-3}$ *at higher energies. Not much difference is observed between 0.5 and 5 micrometers, an indication that there is a lack of track-registering particles below 0.5 million electron volts per nucleon. The Surveyor data are compatible with track results in lunar rocks, provided an erosion rate of* $\sim 10^{-7}$ *centimeter per year is assumed for the latter. The results also suggest a small-scale erosion process in lunar rocks.*

The Apollo 12 spacecraft has returned to earth Surveyor 3 samples that were exposed for 2.6 years on the moon. We present here preliminary results of studies of nuclear tracks in a piece of clear filter glass used to cover the lens of the TV camera from the Surveyor 3 spacecraft. The results give information about low-energy nuclear particles from the sun and provide a basic calibration for nuclear tracks in the surfaces of lunar rocks (*1, 2*).

The TV camera was mounted vertically inside a shroud open on one side (images were obtained from a mirror above the lens). The lens was covered by a horizontal filter wheel. After 2 weeks of operation the clear filter was left directly in front of the shroud opening until recovery.

We recently received a piece of this glass ~ 0.35 cm^2 in area and 0.3 cm thick. A microprobe scan shows that the glass contains a large amount of Pb and smaller amount of K. From the density (3.60 g cm^{-3}) and the index of refraction ($n = 1.61$), we infer that the Pb content must be close to 43 percent (by weight) (*3*). The microprobe also showed a small amount of Mg, presumably from a $\lambda/4$ coating of MgF_2.

The geometry of the glass with respect to the opening was specified as follows (*4*): (i) A reference line $\overline{AB}$ was drawn on the surface of the glass. This line ran from left to right for an observer standing in front of the camera. (ii) A wire was placed perpendicular to the line $\overline{AB}$ at the point where our sample was taken. The wire was then rotated in a vertical plane until it bisected the opening from top to bottom. (iii) A piece of clear plastic was then placed perpendicular to the wire, and the outline of the opening was traced out. Specification of the coordinates in the plane of the plastic (x,z), the elevation of the wire, and the distance from the sample to the x,z reference plane fix the geometry.

The sample was cut into three parts with the first cut made parallel to $\overline{AB}$ at an angle to the exposed surface of 60°. This was done to ensure that the tracks were incident at a steep angle. One piece (section 1) was put in epoxy, polished, and etched (1 percent HF solution) to study the depth dependence. The other pieces were used to study tracks on the exposed surface. Measurements were made with a scanning electron microscope at a depth of from 0 to 30 μm and with an optical microscope starting at a depth of 10 μm. As shown in Fig. 1, the density is $(1.14 \pm 0.06) \times 10^6$ track cm^{-2} at 3.8 ± 1 μm from the surface and drops off rapidly with depth.

The remaining samples of the top surface were given varying treatments in H_2SO_4 and HNO_3 solutions to etch the MgF_2 coating. There are two layers of material covering the glass surface: the MgF_2 coating, which is ~ 1400 Å thick, and a second layer, ~ 0.4 μm thick, with a composition somewhat enriched in Si with respect to the glass. Possibly the second layer is a silane coating used to enhance the adhesion of the MgF_2.

No tracks were found in the MgF_2, although the right etchant may not have been used. When the MgF_2 was removed by etching in HNO_3 at 75°C for 1 hour, the second film was left intact. Subsequent etching in dilute HF gave a high density of shallow pits ($\sim 3 \times 10^8$ cm^{-2}). Shallow pits could also be seen on the glass substrate in areas where the film was broken away. However, similar pits were seen on the bottom, unirradiated portions of the glass and in some areas of a control glass provided by the Jet Propulsion Laboratory of the California Institute of Technology; it is thus unlikely that they are tracks of nuclear particles.

Further etching in HF removed the thick film and gave deep, characteristic track etch pits in the exposed glass surface. These tracks are clearly oriented toward the camera opening (see Fig. 2). The density of these pits is $(8.3 \pm 0.5) \times 10^5$ track cm^{-2}. When corrected for the geometry, this corresponds to a